**International Global Navigation Satellite Systems Association**
**IGNSS Symposium 2020**

Colombo Theatres, Kensington Campus, UNSW Australia
5 – 7 February 2020

# A Measurement Campaign for Cooperative Positioning Architecture Based on GNSS and Local Positioning System

***Jelena Gabela***
Department of Electrical and Electronic Engineering, The University of Melbourne, Australia
jgabela@student.unimelb.edu.au

***Elizabeth Smith***
University of New South Wales/Defence Science and Technology Group, Australia
liz.smith@dst.defence.gov.au

***Shenghong Li***
Data 61, CSIRO, Sydney, Australia
Shenghong.Li@data61.csiro.au

***Allison Kealy***
Department of Geospatial Science, RMIT University, Australia
allison.kealy@rmit.edu.au

***Mark Hedley***
Data 61, CSIRO, Sydney, Australia
Mark.Hedley@data61.csiro.au

***Wei Ni***
Data 61, CSIRO, Sydney, Australia
Wei.Ni@data61.csiro.au

***Andrew Dempster***
University of New South Wales, Sydney, Australia
a.dempster@unsw.edu.au

***Joon Wayn Cheong***
University of New South Wales, Sydney, Australia
cjwayn@unsw.edu.au

## ABSTRACT

Collecting data for testing and validation of Cooperative Positioning (CP) systems is time-consuming and often requires a big bulk of sensors. Therefore, this data is usually simulated to obtain results that validate different CP solutions. Although that is valid, real-world experimental data can, due to generally unpredictable nature (e.g., multipath, random reduction of measurement quality due to used sensors), indicate some issues with CP that

simulated data may not. In this paper, a smaller scale measurement campaign for collecting CP data is described in detail. The benefit of this is the availability of real-world data for algorithm validation with the compromise of having a smaller test area. The measurements were collected in September 2018 in Sydney, Australia, for four pedestrians which were equipped with GNSS receivers, Ultra-Wide Band (UWB) radios and Wireless Ad-hoc System for Positioning (WASP) units. Local Positioning System (LPS) anchors equipped with WASP and UWB units were set up around the data collection area. Experiment design, setup, execution, quality assessment of the data and recommendations for future data collections are presented in the paper. In addition to this, to quantify the performance of the collected data, a comparison of multi-sensor fusion (GPS and local positioning system) and standalone GPS solution for each user is made. Further, integrity availability is assessed for standalone GPS and multi-sensor fusion solution. The performance is assessed under different conditions (e.g., static or dynamic pedestrians, data under the influence of multipath or with the open sky).

**KEYWORDS**: Cooperative Positioning, GNSS, Local Positioning System - LPS, Measurement campaign.

## 1. INTRODUCTION

Cooperative Positioning (CP) is a field of research into using multiple sensors, both fixed and mobile communicating together to establish their collective position. Its application is predominantly in Cooperative Intelligent Transport Systems (CITS) where vehicles communicate with each other and local infrastructure to provide a more accurate and robust position solution.

A lot of literature today in CP uses simulated data to verify and validate their positioning algorithms as it limits the number of errors introduced into the system (Benslimane, 2005; Gabela *et al.*, 2018; Li *et al.*, 2019; Liu *et al.*, 2018; Parker and Valaee, 2007; Steinmetz *et al.*, 2019). This approach has its benefits, such as large data sets, and a high rate of simulation runs to create statistically significant results. The downfall of simulated data is the very thing that makes it appealing for use in research, the lack of realistic random error sources. Algorithms only tested using simulated data may not be able to perform correctly when exposed to real-world data.

Though some literature does use real experimental data (Sheng *et al.*, 2017; Wang *et al.*, 2016). The data sets tend to be limited and only 'represent' a real cooperative vehicle situation. Often, it is necessary for smaller data sets to be extracted from the larger to obtain a period of continuous data operation. This highlights one of the main error sources for real-world experiments, data dropouts. In some cases, however, a combination of the two processes above is used, where real data and simulated data are combined (Fascista *et al.*, 2018; Goel *et al.*, 2018; Soatti *et al.*, 2018). This allows for some controlled errors to be introduced yet still have accurate knowledge of what the data was doing in a realistic scenario.

A data collection activity where real-world CP data is collected and processed to establish the effect of realistic errors on current CP techniques is detailed in this paper. The experiment was a joint undertaking between Melbourne University, University of New South Wales (UNSW), Royal Melbourne Institute of Technology (RMIT) University and the Commonwealth Scientific and Industrial Research Organisation (CSIRO). The focus of this paper is the

description of the measurement campaign which includes a description of the commercial sensors used, the data collection process and the analysis of data availability and quality. Quality of the data is also analysed through a demonstration of the achievable performance in terms of position accuracy and integrity with the real-world data.

The European GNSS Agency report from 2015 (see References) lists model validation as one of the open issues that need to be addressed in terms of a positioning integrity algorithm. As mentioned before, algorithms validated only using the simulated data may not be able to perform correctly when exposed to the specific error sources of the local environments that need to be characterised. Thus, to fully validate a framework one of the objectives needs to be an extensive data collection campaign "aiming to characterise error sources, magnitudes and probabilities for two important GNSS terrestrial application areas: automotive and pedestrian users". This is one of the objectives of the European Commission funded project The Integrity GNSS Receiver (IGNSSRX) (Domínguez *et al.*, 2014). However, extensive data collections for CP can be costly, logistically demanding, time-consuming to plan and hard to organise due to a lot of variables (e.g., number of participants, sensors, organising vehicles, organising data collection area). Thus, this paper proposes a smaller scale data collection with smaller costs, less complicated to organise and less demanding. The data sets collected like this will not be able to fully capture the benefits of an extensive measurement campaign, but it will introduce the realistic random errors which will not result in the optimistic performance estimates for the proposed algorithms.

This paper will highlight the sensors used in Section 2, the data collection process in Section 3 and an evaluation of the performance of the data in Section 4. The conclusion will recommend improvements for future data collection activities to improve data integrity and performance.

## 2. SENSOR DESCRIPTION

During the data collection, three different sensors were used: GNSS receiver, WASP system and UWB system (Figures 1a-c). This section provides some general information about each system and describes the sensors used.

a) b) c)

**Figure 1.** During the measurement campaign, three types of sensors were used: a) GNSS receiver. b) WASP unit. c) UWB unit.

Four Leica Viva GS15 units were used as the mobile GNSS receivers during the campaign.

They were also used to survey the infrastructure nodes in order to determine their precise locations. For this experiment, Navstar GPS and GLONASS signals were recorded, but only Navstar GPS was used for positioning. The GPS positions were post-processed after the experiment using precise ephemeris and Differential GPS (DGPS) corrections to determine the truth trajectories for all users. The GNSS receiver and antenna setup are shown in Figure 1a. More information about the receivers can be found in Leica Geosystems AG brochure (see References).

One of the two types of relative ranging equipment used during this experiment is the Wireless Ad hoc System for Positioning (WASP) developed by CSIRO (Sathyan *et al.*, 2011). The WASP is a software-defined radio that uses Time-Of-Arrival (TOA) to calculate distances between nodes. Time synchronisation issues are eliminated by using round trip ranging to calculate ranges between nodes. The transceiver is a low-cost piece of hardware with a maximum output power of 100mW. It operates in the 2.4 GHz and 5.8 GHz frequency bands; the 5.8 GHz band being the one used for this experiment. This is due to it having less interference and a larger available bandwidth of 125 MHz. Each node can either be a mobile tag that is located on the vehicle or person, or a stationary reference node such as local infrastructure. A server is required to translate the signals from the nodes into a set of positions. The server can be centralised or distributed depending on the requirements for the network. An example node is shown in Figure 1b.

Ultra-Wide Band (UWB) sensors were also used in this experiment (see Figure 1c). Decawave's MDEK1001 Development Kit was used (Decawave product brief, 2017); all of which are capable of being configured as anchors or mobile nodes. As per the system specifications, typically 2D accuracy of <10 cm is achievable with a maximum position estimation rate of 10 Hz. The maximum range that this system can measure is 60 m in Line-of-sight conditions. An example of the relationship between anchors and mobile users is shown in Figure 2. For this experiment, seven anchor nodes and one mobile user tag were used. For alternative UWB sensor types and positioning see; Zandian (2019), which gives an overview of available UWB technologies.

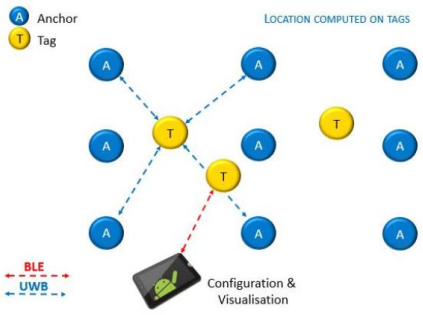


**Figure 2.** An example of the relationship between anchors and mobile users. The connection between them and the android app on a mobile device are shown as well (Decawave product brief, 2017).

## 3. DATA COLLECTION PROCEDURE

As the experiment uses relative ranging devices, the UWB and WASP units required setting up a Local Positioning System (LPS). Thus, a network of 15 anchor nodes (i.e., infrastructure nodes) was set up, as shown in Figure 3. Out of 15 anchors which were all equipped with WASP units, seven anchors were also equipped with the UWB units. The coordinates of the anchors

were determined with sub-centimetre level precision after post-processing GPS data. Given the idea of collecting real-world data on a smaller scale, the anchor nodes were set up on an open-sky area of about *30 m·60 m*. An example of the infrastructure node is shown in Figure 4a.

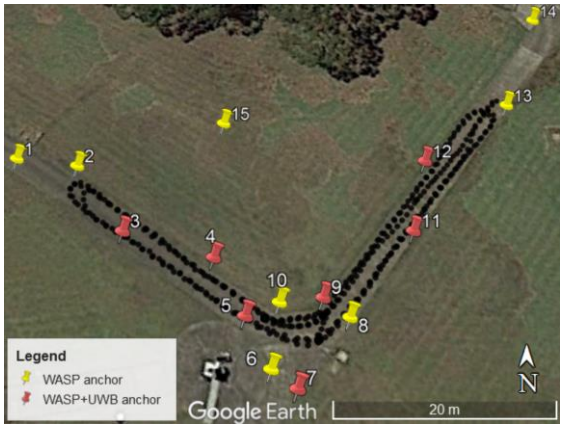


**Figure 3.** Data collection area with anchors. Yellow anchors are equipped with WASP. Red anchors are equipped with both the WASP and UWB sensors. An example of the trajectory is shown in black.

In this measurement campaign, there were four users collecting data. All users collected GNSS data, WASP relative ranges to the infrastructure (Peer-to-Infrastructure P2I) and WASP relative ranges to other users (Peer-to-Peer P2P). In addition to this, User 2 measured UWB relative ranges to the infrastructure nodes (i.e., UWB P2I). Thus, all users were equipped with one GNSS receiver and one WASP unit (User 2 was also equipped with UWB radio). User 2 is shown in Figure 4b. The ground truth trajectories for all users have been determined with sub-centimetre level precision by post-processing the dual-frequency GPS.


a) b)

**Figure 4.** Sensor set-up for a) an example of the infrastructure node. b) User 2.

Measurement campaign consisted of three different experiments: static, dynamic and dynamic+multipath. During the static experiment, all users were stationary in the area between anchors 5-10 for almost *3 min* (see Figure 5a). The static experiment was followed by the dynamic experiment where the users walked along the improvised road segment with an average speed of *1* $ms^{-1}$ for *6.5 min* (see Figures 5b and 5c). The final executed experiment involved provoking the multipath in an otherwise open area without big sources of multipath.

Thus, this experiment is named dynamic+multipath. During this experiment, possible multipath sources were installed along one part of the trajectory. As shown in Figure 5d, big reflective panels and vehicles were used. The users again walked with an average speed of *1 ms*$^{-1}$ for a little over *6 min*.

a) b) c) d)

**Figure 5.** Measurement campaign can be divided into three different experiments. a) Experiment 1: static. b) Experiment 2: User 2. c) Experiment 2: Dynamic. d) Experiment 3: Dynamic+multipath.

### 3.1 Time Synchronisation

The three positioning systems (WASP, UWB, and GNSS) used in the experiments are independent of each other and use different clocks. Therefore, the measurements obtained from these systems need to be time synchronised for sensor fusion and CP. This is achieved by estimating and compensating the relative clock offsets between these systems. The measurements of each system can be denoted as $\left\{m_n^S, t_n^S\right\}_{n=1}^{N_S}$, where $S \in \{WASP, UWB, GNSS\}$, and $m_n^S$ are the (pseudo)range measurements obtained at time $t_n^S$. Since the time stamps $t_n^S$ are recorded using unsynchronised clocks, they are subject to clock offset and clock skew. The effect of clock skew on $t_n^S$ is negligible due to the short duration of the experiments (less than 10 minutes). Thus, the focus is on estimating the relative clock offsets between these systems, which is achieved by shifting the estimated target trajectories along the timeline so that they are aligned. Specifically, the target positions $x_n^S$ are first estimated from $m_n^S$, thus the clock offset between any two systems $S_1$ and $S_2$ is given by

$$t_{S_1-S_2} = \min_{t} \sum_{n=1}^{N_{S_1}} \left\| x_n^{S_1} - x_{m(n,t)}^{S_2} \right\|^2 \tag{1}$$

where

$$m(n,t) \triangleq \min_{m} \left| t_n^{S_1} + t - t_m^{S_2} \right| \tag{2}$$

gives the index of measurement for the system $S_2$ that is closest to the $n^{\text{th}}$ measurement of the system $S_1$ in the time given a clock offset of $t$. Here, the WASP system was chosen as a reference. The relative clock offsets of the UWB system and GNSS system were estimated and compensated, such that all timestamps refer to the same clock.

### 3.2 Data Availability

This section provides an overview of the data availability for all LPS P2I and P2P measurements. The WASP ranging measurements to all 14 infrastructure nodes and 3 users were made at a ping frequency of approximately *10 Hz*. The ping frequency of the UWB ranging measurements from the User 2 to all 7 infrastructure nodes was around *9.8 Hz*. GNSS data were collected with a frequency of *1 Hz*. In this paper, only GPS data was used, although GLONASS data were collected as well. Data availability is shown for *1 Hz* frequency.

Figure 6 shows the availability of the WASP P2I measurements for all users across all experiments. User 1 and 3 experience more outages during the dynamic experiment (orange colour in the graph) than in the dynamic+multipath experiment (yellow colour in the graph). For now, it is unknown why this occurs and what will be the effect of this on the positioning/integrity monitoring performance. In terms of measurement availability, WASP P2I measurements seem to be very stable as the number of available ranges rarely goes under *12*. It should be noted, although 15 anchors were set up, one of the anchors in the intersection was not functioning. The availability of the WASP P2P ranges is shown in Figure 7. Similarly, to the WASP P2I ranges, in terms of availability, WASP measurements seem to be stable as the number of P2P measurements rarely goes under *2*.

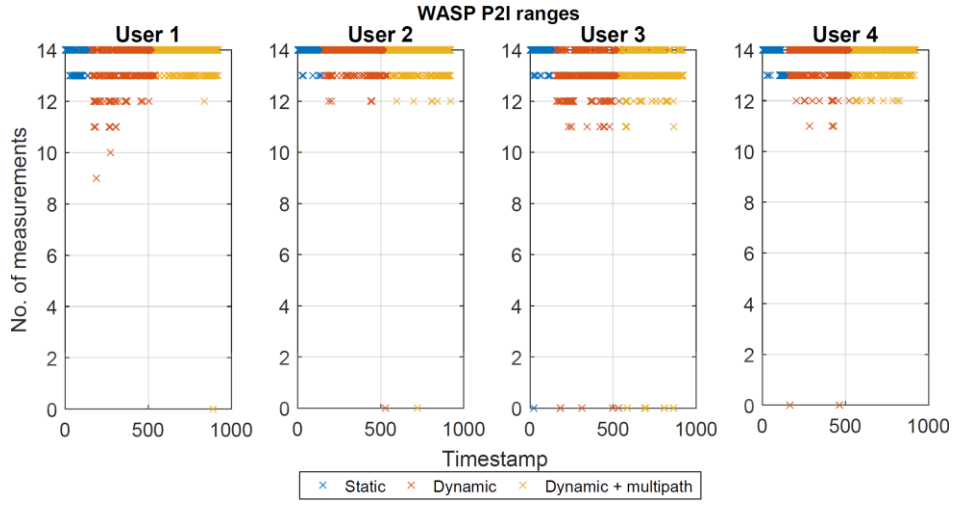


**Figure 6.** Availability of WASP P2I measurements for all users and all experiments.

User 2 was the only one equipped with a UWB radio. Thus, the availability of the UWB P2I relative ranges is shown in Figure 8 (green colour). Although there were seven anchors equipped with UWB units, the maximum number of anchors User 2 was able to communicate with was four across all the experiments. The rate of data outage is little under *50%* of the time. Furthermore, Figure 8 shows the availability of all used sensors for User 2, including GPS measurements, across all the experiments. As expected, the number of measurements seems to be the most stable during the static experiments. GPS data is also stable in terms of availability, where more outages are experienced when multipath is provoked.

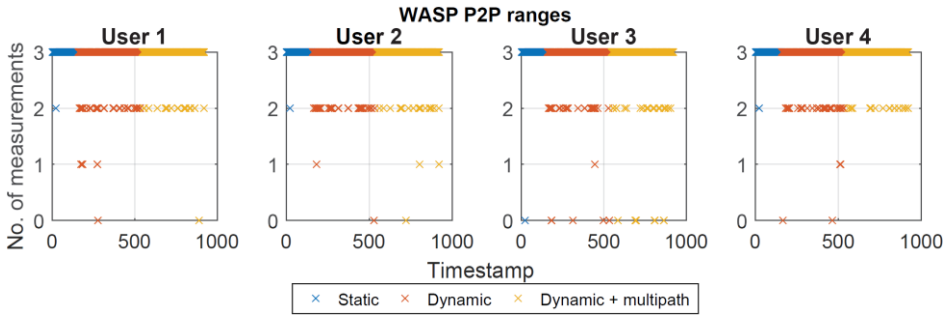


**Figure 7.** Availability of WASP P2P measurements for all users and all experiments.

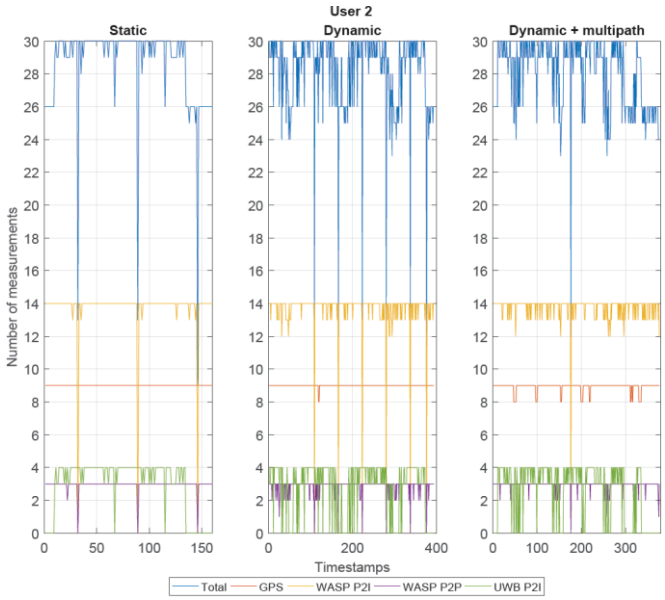


**Figure 8.** The overall measurement availability during all experiments for User 2.

### 3.3 Data Quality

This section presents the analysis of the LPS ranging errors for all users and all anchor nodes across all the experiments. The range errors are estimated by comparing the measured ranges and range measurements calculated from the ground truth.

Firstly, WASP P2I ranges are analysed (see Figure 9). The x-axis of the graph represents every infrastructure node. Generally, the best ranging accuracy was achieved for all anchors during the static experiment. It was expected that the ranging accuracy would decrease when multipath is provoked in comparison to the dynamic experiment. However, this was not the case. Only

User 2 and 3 show the expected accuracy deterioration. User 1 shows that the ranging accuracy improves during the dynamic+multipath experiment (in comparison to the dynamic experiment). The average accuracy of WASP P2I ranging for the static experiment is *0.2 m*. The average accuracy for the dynamic experiment is *0.6 m*. However, it should be mentioned that the average ranging accuracy for User 1 is *1.3 m*, Users 2 and 3 is around *0.3 m*, and for User 4 is *0.5 m*. That difference is caused by the larger outliers recorded by Users 1 and 4 (maximum around *90 m* in comparison to the maximum *60 m* for User 2 and 3). However, it is unknown why this happened. It may be due to some device-specific reasons or due to an error made during the data collection. The average error for dynamic+multipath experiment is *0.5 m*. On average, User 1's ranging error is *0.4 m*, *0.7 m* for User 2 and *0.5 m* for Users 3 and 4. Average errors confirm the results shown in Figure 9: User 1 performs better during dynamic+multipath experiment, User 2 and 3 perform as it was expected, and User 4 performs similarly during both the experiments.

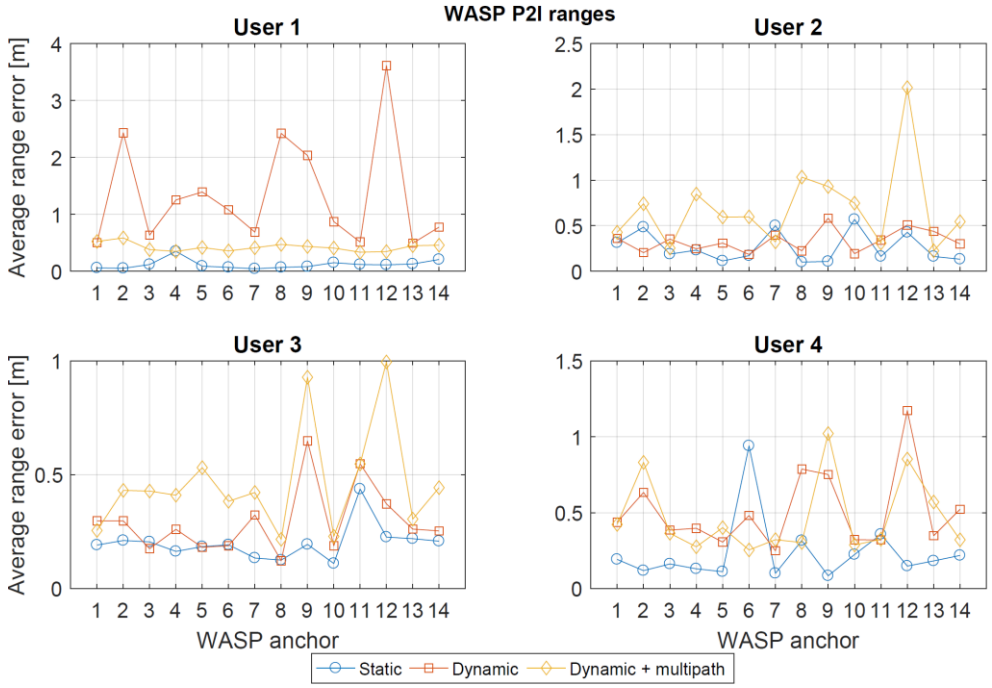


**Figure 9.** The average error of WASP P2I measurements for all anchors (x-axis). The average error is shown for all users as well as all experiments.

Figure 10 shows the average accuracies of WASP P2P ranges (i.e., ranges between users). If the average ranging error is equal to *0 m*, this indicates it is the communicating node (i.e., if the communicating node is User 1, measurement to User 1 does not exist. Thus, it is shown with *0 m* average error). The average accuracy of WASP P2P for all users is around *0.2 m* (same as P2I). During the dynamic experiments, the average ranging error is estimated to be *1.5 m*, and for the dynamic+multipath experiments, it is *1.1 m*. Again, the overall average accuracy is probably affected by the larger outliers present in the dynamic experiment data (maximum outlier is *104 m* compared to maximum dynamic+multipath outlier of *66 m*).

Lastly, the UWB P2I ranging errors are analysed for every anchor node (x-axis) (see Figure 11). The average ranging error of *0.2 m* is observed for dynamic experiment and *1.0 m* for the dynamic+multipath experiment. Average of *1.0 m* is largely due to anchor node 4. Anchor node 4 was positioned next to the vehicles and across from the reflective panes (see Figures 3

and 5d). However, given that the anchor nodes 3 and 5 did not measure similar outliers, it is possible a different error source could have affected anchor node 4.

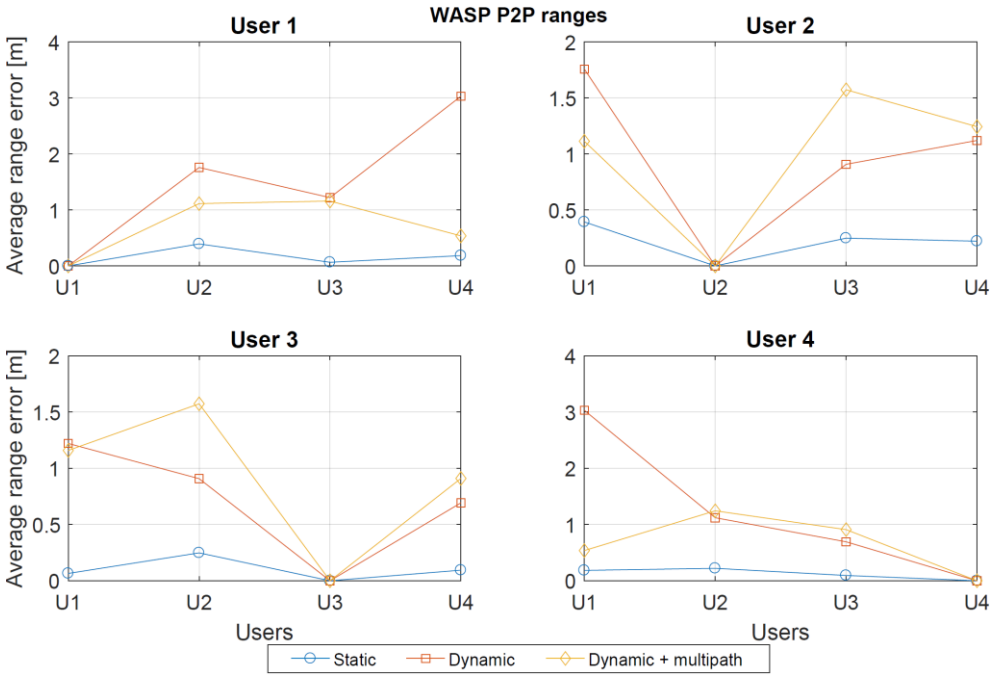


**Figure 10.** The average error of WASP P2P measurements for all users (x-axis). The average error is shown for all users as well as all experiments.

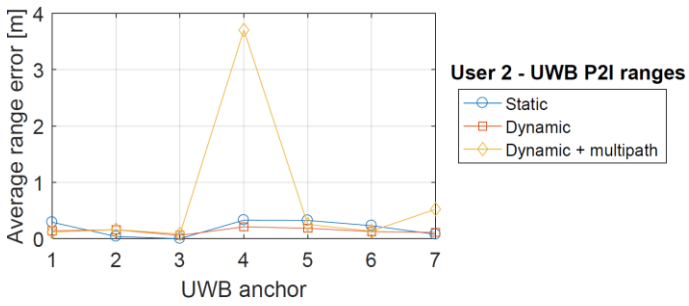


**Figure 11.** The average error of UWB P2I measurements for all anchors (x-axis). The average error is shown for User 2 for all experiments.

## 4. PERFORMANCE DEMONSTRATION

To demonstrate the performance of the collected data, the Extended Kalman Filter (EKF) and Weighted Least Squares Receiver Autonomous Integrity Monitoring (WLS RAIM) algorithms are integrated. To do this, GPS and WASP P2I data (i.e., relative ranges measured from users to infrastructure) are fused (i.e., GPS+WASP). Given the focus of this paper, those algorithms are not detailed here.

The positioning framework used here is presented in detail in Gabela *et al.* (2018). When implementing these algorithms, process and measurement noise were assumed to be zero-mean Gaussian with the standard deviations of *1* $ms^{-2}$ for the acceleration noise, *1 m* for the user clock bias noise, *5.1 m* for the GPS pseudorange measurements and *1 m* for the WASP relative ranges. Smith *et al.* (2018) present the used WLS RAIM in detail. This algorithm was first explained

in Bruckner (2010).

Monitoring the integrity of the estimated positions of different road users has become increasingly important with the development of the Intelligent Transport Systems (ITS) due to the requirements of different applications (e.g., anti-collision systems, tolling, emergency services). Integrity can be defined as "a general performance feature referring to the level of trust a user can have in the value of a given position or velocity as provided by a location system" (European GNSS Agency, 2015). Due to the specificity of different road applications, a uniform set of integrity monitoring requirements is not defined and agreed on, as it is the case in civil aviation (Ochieng *et al.*, 2003). Thus, in this paper, requirements for Payment-Critical Applications (PCA) (e.g., tolling) specified in the European GNSS Agency's report (2015), have been used. Required Horizontal Alarm Limit (HAL) is *20 m* and the integrity risk is required to be $1 \cdot 10^{-5}$. In general, integrity risk defines the probability that at any moment, the Positioning Error (PE) will exceed the estimated Protection Level (PL). Given that the PE is unknown, it can be said that PL assures the user that the estimated position is within the PL limits with the probability of failure equal to integrity risk. Further, for integrity to be available, the estimated PL cannot be larger than the AL. In this paper, horizontal PE and PL are estimated. Thus, notations HPE, HPL and HAL are used.

Figure 12 presents the integrity and the positioning performance in form of the Stanford diagram (more in Smith *et al.*, 2018) which classifies the integrity availability based on the fulfillment of the requirements that HPE needs to be smaller than the HPL, and HPL needs to be smaller than the HAL. The results for only two users are shown: User 1 (Figures 12a,c,e) and User 2 (Figures 12b,d,f).

The performance in the static experiment is similar for both users (Figures 12a and 12b). The average HPE is *0.13 m* and *0.21 m* for User 1 and 2, respectively. The standard deviation of HPE is around *0.10 m* for both users. Similar performance is observed for the other two users. As expected, the best integrity availability is achieved in the static experiment where both users meet the integrity requirements about *98%* of the time (i.e., integrity is available).

The dynamic experiment shows the degradation of the integrity levels achieved in the static experiment (Figures 12c and 12d). However, the performance of users is no longer similar. Integrity is available *77%* of the time for User 1 with the appearance of the misleading and hazardously misleading information *14%* and *5%* of the time, respectively. Unlike User 1, hazardously misleading information does not occur for User 2. Integrity is available *93%* of the time and the misleading information occurs 3% of the time. Given that the data for both users were collected in the same conditions using the same type of instruments in a short span of time, it was expected that the integrity availability would be similar. Average HPE is *3.65 m* and *0.75 m* with standard deviations of *7.26 m* and *1.87 m* for User 1 and 2, respectively. The large standard deviation of HPE for User 1 indicates that large outliers were present in the measured data that affected the average HPE. This conclusion is confirmed by the WASP P2I ranging quality assessment (see Section 3.3) where large outliers were present in User 1's data. Here, the position estimate would probably benefit from a Fault Detection and Exclusion (FDE) algorithm (an example of FDE can be found in Smith *et al.*, 2018).

Figures 12e and 12f show the performance of User 1 and 2 in the dynamic+multipath experiments. User 2 experienced further degradation of integrity availability (*90%*) and an increase of misleading information to *6%* and hazardously misleading information to *2%*. Average HPE further increased to *1.83 m* with a standard deviation of *5.04 m*. However,

User 1's integrity availability was increased to *97%* with a decrease of misleading information to *1%*. Hazardously misleading information did not occur during the dynamic+multipath experiment. In the case of User 1, average HPE is *0.60 m* and the standard deviation is *0.98 m*.

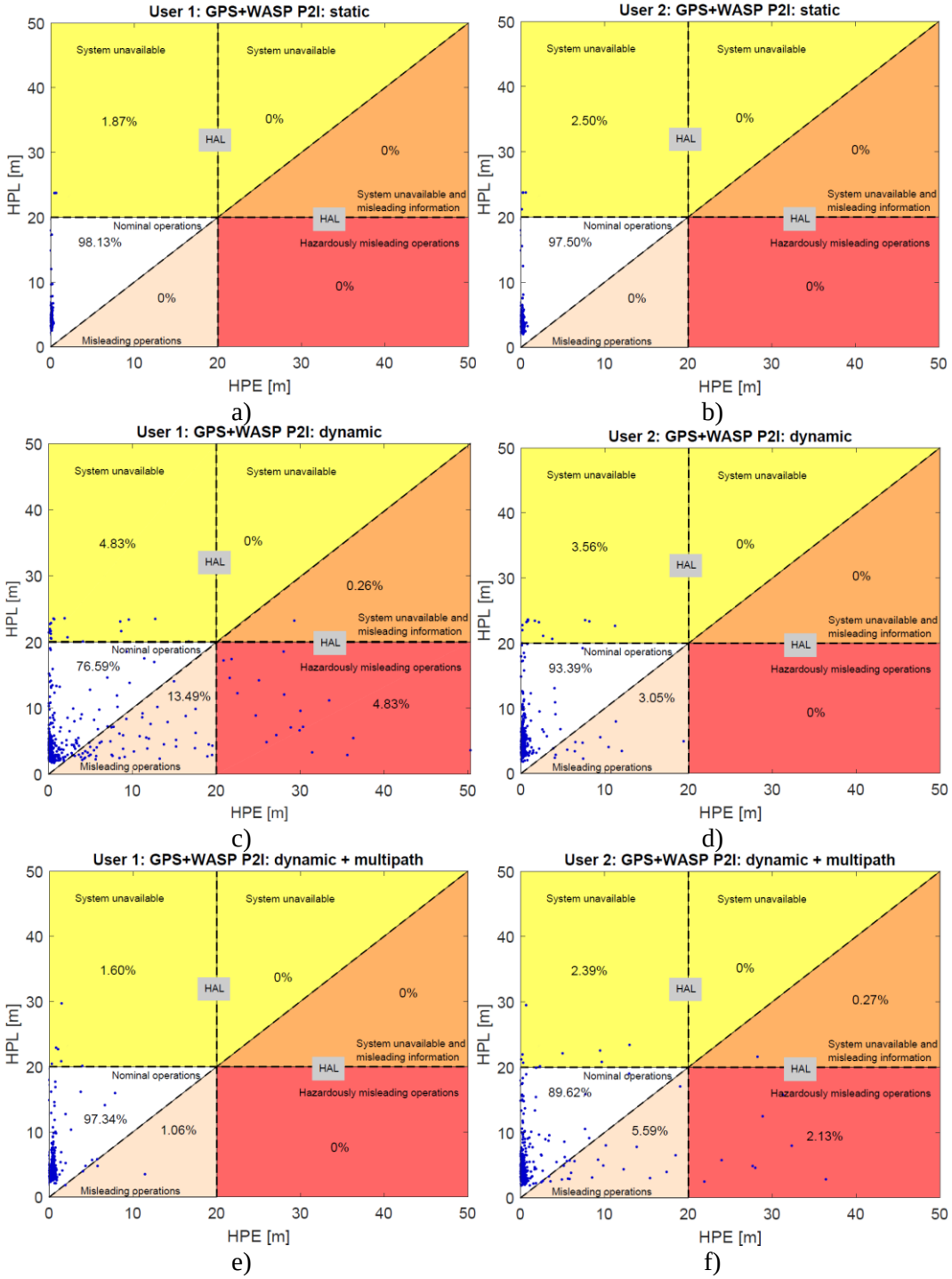


**Figure 12.** Integrity availability for a) User 1 in the static experiment. b) User 2 in the static experiment. c) User 1 in the dynamic experiment. d) User 2 in the dynamic experiment. e) User 1 in dynamic+multipath experiment. f) User 2 in dynamic+multipath experiment.

The performance of the other two users is similar to the performance of User 1 and 2. User 3 shows the same 'behaviour' as User 2 and User 4 shows the same 'behaviour' as User 1. Thus, the results just for two users were shown. During data collection, the main hypothesis was that

the performance will gradually deteriorate with new experiments. The best performance was expected when the users were static, and the worst performance was expected when the users were dynamic in addition to operating in conditions of provoked multipath. User 2 and 3 clearly show this progression. However, User 1 and 4 behave contradictory to the hypothesis previously stated. These results were anticipated based on the average ranging errors shown in Figures 9 and 10. Given that only four users participated in the experiments, a conclusion cannot be made about the source of these errors or which pair of users presents realistic performance.

In addition to the multi-sensor fusion solution, the performance of the standalone GPS data is tested. Table 1 presents, for each user and for every experiment, change in standard deviations and maximum HPE. The average HPE for all users was similar (*2.5 m - 2.7 m*). However, the most important information can be seen in the change of standard deviations and maximum HPE. The performance for all users within a specific experiment (see Table 1 columns) is similar with small variations from user to user. This is expected due to the use of the same GNSS receivers and collection of data in a short period of time on a small area in the same conditions. However, the change is visible for specific users between different experiments (See Table 1 rows). Here, a clear increase of standard deviations and maximum HPE is visible from the static experiment to the dynamic+multipath experiment, for every user. Figure 8 shows that the GPS availability was stable with nine satellites being visible at almost all times. As mentioned before, this data was collected in the same conditions with the same sensors. Thus, it is probable that deterioration of the standard deviation and increase of maximum HPE between static and dynamic experiments was caused by users being dynamic in the second experiment. In the second case, where users were dynamic in both experiments, it is probable that the deterioration of the standard deviation and increase of maximum HPE was caused by the provoked multipath in the third experiment. It should be noted, that for specified integrity requirements (HAL *20 m* and integrity risk $1 \cdot 10^{-5}$), *100%* of the time for all users in all experiments, integrity is unavailable for standalone GPS. Although the HPE is within HPL, due to dependence of WLS RAIM on the number of measurements, HDOP and measurement variance, HPL estimate is too conservative. Thus, integrity is not available. Given that all users experience the same results for standalone GPS solution, which is not the case for multi-sensor fusion results, it is reasonable to conclude that the unexpected results are not caused by GPS but are caused by the outliers in WASP data.

| | | Static | Dynamic | Dynamic + multipath |
|---|---|---|---|---|
| User 1 | Std.dev. [m] | 0.11 | 0.14 | 0.35 |
| | Max HPE [m] | 2.68 | 2.96 | 4.75 |
| User 2 | Std.dev. [m] | 0.11 | 0.13 | 0.47 |
| | Max HPE [m] | 2.68 | 2.91 | 4.71 |
| User 3 | Std.dev. [m] | 0.11 | 0.14 | 0.46 |
| | Max HPE [m] | 2.64 | 3.05 | 5.03 |
| User 4 | Std.dev. [m] | 0.11 | 0.15 | 0.52 |
| | Max HPE [m] | 2.72 | 3.10 | 5.21 |

**Table 1.** Standalone GPS performance for all users

## 5. CONCLUSION

This paper has presented the measurement campaign carried out as a joint effort between the Melbourne University, UNSW, RMIT University and the CSIRO. In collaboration, data sets were collected which will be used by the group for initial validation of developed positioning

and integrity monitoring algorithms. Gabela *et al.* (2019) is the first publication which has used the presented data for the experimental study of the effect of linear approximations and Gaussian noise assumptions on the positioning performance. In future, the authors will use the data set for validation of various integrity monitoring and FDE algorithms. This paper offers an overview of the collected data with detailed quality assessments of the LPS measurements. The results show that the sensors used in the measurement campaign are reliable in terms of availability and generally offer sub-meter ranging accuracy. Furthermore, although large outliers can occur, it is expected that the FDE algorithm would be able to detect and exclude those outliers given the high data availability. Because the small scale real-world data was collected, the proposed algorithms will be tested on the data that consists of random and large outliers which should benefit those algorithms in terms of robustness.

In future, the authors would suggest a couple of changes that could be implemented in such a data collection exercise. Planning and getting familiar with the equipment is very important, thus, to avoid issues (e.g., instrument malfunction) in the field which need to be solved quickly and often with a lot of compromises (e.g., using a different less precise instrument). Thus, it is imperative to spend a couple of days on planning and confirming with all participants what needs to be done. Although the main idea is to lower different costs by having a smaller scale measurement campaign, once in the field, as much data as possible need to be collected. This measurement campaign would have benefited had all the experiments been conducted multiple times at different times of the day. That would possibly have helped with issues described in the paper. Lastly, one of the biggest issues when organising measurement campaigns is the lack of sensors that are available for data collection for CP systems. Thus, the cooperation between different research groups is beneficial, not just in combining various sensors but also in producing a data set that can be used for different purposes.

## ACKNOWLEDGEMENTS

The authors thank UNSW School of Civil & Environmental Engineering and Dr Craig Roberts for lending the four GNSS receivers used for data collection.

## REFERENCES

Benslimane A (2005) Localization in Vehicular Ad Hoc Networks, *2005 Systems Communications (ICW'05, ICHSN'05, ICMCS'05, SENET'05)*.

Bruckner DC (2010) On the Treatment of Noise and Conspiring Bias in Dual-Frequency Differential Global Navigation Satellite Systems, *Ph.D. Thesis*, Russ College of Engineering and Technology of Ohio University, Athens, Ohio, USA.

Decawave product brief (2017), available online: https://www.decawave.com/mdek1001/productbrief/ (accessed: 8 Dec 2019).

Domínguez E, Seco-Granados G, Salcedo J, Egea D, Aguado E, Lowe D, Naberezhnykh D, Dovis F, Boyero JP, Fernandez I (2014) Characterization of GNSS Integrity Threats in Terrestrial Applications Using Real Signal Captures, *Proceedings of the 27th International Technical Meeting of The Satellite Division of the Institute of Navigation (ION GNSS+ 2014)*, Tampa, Florida, USA, pp. 954-966.

European GNSS Agency (2015) Report on the Performance and Level of Integrity for Safety and Liability Critical Multi-Applications, *European GNSS Agency report*, available online: https://www.gsa.europa.eu/sites/default/files/calls_for_proposals/Annex%202.pdf (accessed: 8 Dec 2019)

Fascista A, Ciccarese G, Coluccia A, Ricci G (2018) Angle of Arrival-Based Cooperative Positioning for Smart Vehicles, *IEEE Transactions on Intelligent Transportation Systems*, 19(9): 2880-2892.

Gabela J, Goel S, Kealy A, Hedley M, Moran W, Williams S (2018) Cramér Rao Bound Analysis for Cooperative Positioning in Intelligent Transportation Systems, *Proceedings of the International Global Navigation Satellite Systems Association - IGNSS Symposium 2018*, Sydney, Australia.

Gabela J, Kealy A, Li S, Hedley M, Moran W, Ni W, Williams S (2019) The Effect of Linear Approximation and Gaussian Noise Assumption in Multi-Sensor Positioning Through Experimental Evaluation, *IEEE Sensors Journal* 19(22): 10719-10727.

Goel S, Gabela J, Kealy A, Retscher G (2018) An Indoor-Outdoor Cooperative Localization Framework for UAVs, *Proceedings of the International Global Navigation Satellite Systems Association - IGNSS Symposium 2018*, Sydney, Australia.

Kealy A, Retscher G, Gabela J, Li Y, Goel S, Toth CK, Masiero A, Błaszczak-Bąk W, Gikas V, Perakis H, Koppanyi Z, Grejner-Brzezinska D (2019) A Benchmarking Measurement Campaign in GNSS-denied/challenged Indoor/Outdoor and Transitional Environments, *Proceedings of the FIG Working Week*, Hanoi, Vietnam, paper 9837, 19 p, available online: http://fig.net/resources/monthly_articles/2019/kealy_etal_july_2019.asp (accessed: 8 Dec 2019).

Leica Geosystems AG, Leica Viva GNSS GS15 receiver Datasheet, available online: https://w3.leica-geosystems.com/downloads123/zz/gpsgis/viva%20gnss/brochures-datasheet/leica_viva_gnss_gs15_receiver_ds_en.pdf (accessed: 8 Dec 2019).

Li W, Xiong Z, Sun Y, Xiong J (2019) Cooperative positioning algorithm of swarm UAVs based on posterior linearization belief propagation, *Proceedings of the 2019 IEEE 3rd Information Technology, Networking, Electronic and Automation Control Conference (ITNEC)*, Chengdu, China, pp. 1277-1282.

Liu J, Rizos C, Cai BG (2018) Integrity Monitoring of Vehicle Positioning using Cooperative Measurements under Connected Vehicles Environments, *Proceedings of the International Global Navigation Satellite Systems Association - IGNSS Symposium 2018*, Sydney, Australia.

Ochieng WY, Sauer K, Walsh D, Brodin G, Griffin S, Denney M (2003), GPS Integrity and Potential Impact on Aviation Safety, *The Journal of Navigation* 56: 51-65.

Parker R, Valaee S (2007) Cooperative Vehicle Position Estimation, *2007 IEEE International Conference on Communications*, Glasgow, UK, pp. 5837-5842.

Sathyan T, Humphrey D, Hedley M (2011) WASP: A system and algorithms for accurate radio localization using low-cost hardware, *IEEE Transactions on Systems, Man, and Cybernetics, Part C (Applications and Reviews)*, 41(2): 211-222.

Shen F, Cheong JW and Dempster AG (2017) A DSRC Doppler/IMU/GNSS Tightly-coupled Cooperative Positioning Method for Relative Positioning in VANETs, *The Journal of Navigation*, 70(1): 120-136.

Smith E, Knight M, Dempster A, Cheong JW (2018) Integrity Capability of Standalone GPS, *Proceedings of the International Global Navigation Satellite Systems Association - IGNSS Symposium 2018*, Sydney, Australia.

Soatti G, Nicoli M, Garcia N, Denis B, Raulefs R, Wymeersch H (2018) Implicit Cooperative Positioning in Vehicular Networks, *IEEE Transactions on Intelligent Transportation Systems*, 19(12): 3964-3980.

Steinmetz E, Emardson R, Brännström F, Wymeersch H (2019) Theoretical Limits on Cooperative Positioning in Mixed Traffic, IEEE Access, 7: 49712-49725.

Wang J, Gao Y, Li Z, Meng X, Hancock CM (2016) A Tightly-Coupled GPS/INS/UWB Cooperative Positioning Sensors System Supported by V2I Communication, *Sensors*, 16(7), 944.

Zandian R (2019), Ultra-wideband Based Indoor Localization of Mobile Nodes in ToA and TDoA Configurations, *Ph.D. Thesis*, Faculty of Technology of University of Bielefeld, Bielefeld, Germany.